

DEM GENERATION FROM ASTER SATELLITE DATA FOR GEOMORPHOMETRIC ANALYSIS OF CERRO SILLAJHUAY, CHILE/BOLIVIA

Ulrich Kamp

Department of Geography
DePaul University
990 W Fullerton Ave, Chicago, IL 60614-2458, U.S.A.
ukamp@depaul.edu

Tobias Bolch

Department of Geography
University of Erlangen-Nuremberg
Kochstr. 4/4, 91054 Erlangen, Germany
tbolch@geographie.uni-erlangen.de

Jeffrey Olsenholler

Department of Geography and Geology
University of Nebraska – Omaha
6001 Dodge Street, Omaha, NE 68182-0199, U.S.A.
bishop@data.unomaha.edu

ABSTRACT

Digital elevation models (DEMs) are increasingly used for visual and mathematical analysis of topography, landscapes and landforms, as well as modeling of surface processes. A DEM of Cerro Sillajhuay, a volcano in the Andes of Chile/Bolivia, was developed from ASTER (Advanced Spaceborne Thermal Emission and Reflection Radiometer) satellite data. The original 30-m DEM was generated by using tie points, and was finally re-sampled to 15 m to exploit full ortho-image resolution. Five geomorphic parameters, which are useful to identify and describe geomorphologic forms and processes, were extracted using the software ArcInfo and ArcView: elevation, aspect, slope angle, vertical curvature, and tangential curvature. Although the elevation values are slightly to low in altitudes above 5500 m asl., the ASTER DEM is useful for an interpretation of the macro- and mesorelief, and provides the opportunity for mapping especially at medium scales (1:100,000 and 1:50,000).

INTRODUCTION

Digital elevation models (DEMs) are increasingly used for visual and mathematical analysis of topography, landscapes and landforms, as well as modeling of surface processes (Bishop & Shroder 2000, Dikau et al. 1995, Giles 1998, Millaresis & Argialas 2000, Tucker et al. 2001). DEMs play also an important tool for the analysis of glaciers and glaciated terrains (Baral & Gupta 1997, Duncan et al. 1998, Etzelmüller & Sollid 1997, Lodwick & Paine 1985, Sidjak & Wheate 1999). Bishop et al. (2001) used a DEM of Nanga Parbat to map glaciers in the rough mountain terrain of the western Himalayas.

A DEM offers the most common method for extracting vital topographic information and even enables the modeling of flow across topography, a controlling factor in distributed models of landform processes (Dietrich et al. 1993, Desmet & Govers 1995, Kirkby 1990). To accomplish this, the DEM must represent the terrain as accurately as possible, since the accuracy of the DEM determines the reliability of the geomorphometric analysis. Currently, the automatic generation of a DEM from remotely sensed data with sub-pixel accuracy is possible (Krzystek 1995).

DEMs can be generated from stereo satellite data derived from electro-optic scanners such as ASTER (Advanced Spaceborne Thermal Emission and Reflection Radiometer). The ASTER sensor offers simultaneous along-track stereo-pairs, which eliminate variations caused by multi-date stereo data acquisition. Only some results have been published in peer-reviewed literature about using ASTER data yet, mostly on simulated ASTER data (Abrams and Hook 1995, Shi 2001, Welch et al. 1998), or on the potential of using ASTER data in the future (Raup et al. 2000). Wessels et al. (2002) used ASTER data for analyzing supraglacial lakes at Mt. Everest. Cheng & Bean (2002) published first results about the generation of ASTER DEMs for Afghanistan.

This paper presents a DEM derived from ASTER satellite data of the Cerro Sillajhuay in the Andes of Chile/Bolivia. Fieldwork at the Cerro Sillajhuay was conducted only on the Chilean side during March and

April 1998 and focused on geomorphological mapping after Kneisel et al. (1998) and Schröder & Makki (1998) with special respect to geomorphological processes as well as glacial and periglacial forms above 4300 m asl. (Bolch & Schröder 2001). Aerial photographs with a resolution of 2,5 m from 1961 were used for orientation and to monitor the geomorphological mapping. As fieldwork was not possible on the Bolivian side, a detailed, realistic geomorphological mapping of the entire study area is only possible with the help of DEM data.

STUDY AREA

Cerro Sillajhuay (5982 m asl., 19°45' S / 68°42' W) is located in the Andes of Chile/Bolivia, and represents the highest peak of the Andes between 19 and 21 degrees south (Fig. 1). The stratovolcano is in a horst running crosswise to the main north-south orientation of the main Andes ridge as a result of tectonic stress during uplift of the western Cordillera. It rises ~2000 m above the surrounding plain (Fig. 2), and is surrounded by several other volcanos. The median altitude of the massif is ca. 5030 m asl., and most of the terrain lies between 4750 and 5250 m asl. The ca. 3700-m high Salar de Coipasa and Salar de Uyuni on the Bolivian side represent the local erosion level. From here, the pediments smoothly slope up to the Cerro Sillajhuay massif, and only isolated hills break through the generally flat terrain. The massif itself is deeply incised by steeply sloping valleys. For example, the 2-km long Rio Blanco Valley ascends ca. 1100 m from mouth to peak. The ridge of the entire massif is more or less complete, and from here the relief plunges down to the valleys. In the southeast of the volcano lies Cancosa Basin at 3900 m asl., which was formerly covered by a lake (Schröder et al. 1999).

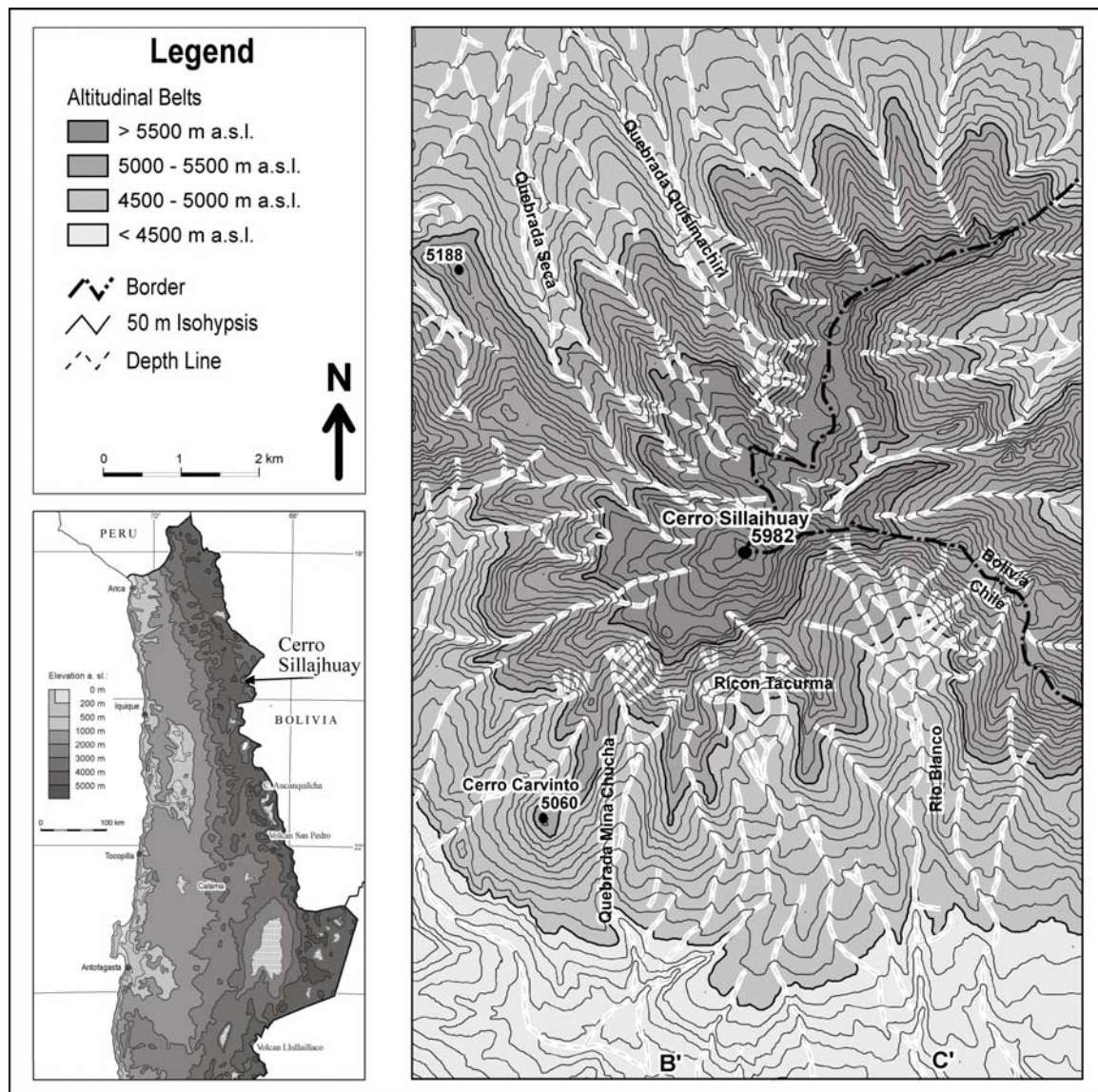


Fig. 1: Location map of the study area in the Andes of Chile/Bolivia.

The study area is part of the Atacama, which is the driest part of the Andes; precipitation occurs in summer. Bolch & Schröder (2001) assume a precipitation of ca. 200 mm in 4500 m asl., and 300-400 mm in 5000 m asl. Cerro Sillajhuay itself is characterized by a local mountain climate with high diurnal variations in temperature and frequent days with frost-thaw-cycles. Discharge is orientated to the interior in the east. Vegetation cover is extreme sparse; grasses and shrubs are dominating and only isolated trees occur.



Fig. 2: View over the Cancosa Basin to Cerro Sillajhuay, a 5982-m high stratovolcano in the Atacama, one of the driest parts of the Andes. See Fig. 4a for comparison with the ASTER DEM simulation.

ASTER INSTRUMENT AND DATA SET

ASTER is a high-spatial-resolution, multispectral imaging system flying aboard TERRA, a satellite launched in December 1999 as part of NASA's Earth Observing System (EOS). An ASTER scene covering 61.5-km x 63-km contains data from 14 spectral bands. ASTER is comprised of three separate instrument subsystems representing different ground resolutions: three bands in the visible and near infrared spectral range (VNIR, 0.5-1.0 μm) with 15 m spatial resolution, six bands in the shortwave infrared spectral range (SWIR, 1.0-2.5 μm) with 30 m resolution, and five bands in the thermal infrared spectral range (TIR, 8-12 μm) with 90 m resolution. In the VNIR one nadir-looking (3N, 0.76-0.86 μm) and one backward-looking (3B, 27.7° off-nadir) telescope provide black-and-white stereo images, which generate an along-track stereo

image pair with a base-to-height ratio of about 0.6. The potential accuracy for the DEM from ASTER could be on the order of ± 7 to ± 50 m (RMSE_z). ASTER is capable of recording 771 digital stereo pairs per day, and cross-track pointing out to 136 km allows viewing of any spot on Earth at least once every sixteen days.

One ASTER-level 1A raw data scene, acquired on May 28, 2001, was downloaded directly from the USGS EROS Data Center (EDC) EOSDIS Core System (ECS). Fortunately, the Cerro Sillajhuay is located in the center of this image, which is absolutely cloud-free.

DEM GENERATION AND 3D-VISUALIZATION

ASTER scenes are distributed in a data format called HDF-EOS, which can be imported by the software OrthoEngine as part of the Geomatica 8.2 package from PCI Geomatics. Using this software, DEMs can be generated automatically. For DEM extraction only the VNIR nadir and backward images (3N and 3B) are used.

Al-Rousan et al. (1997) gave a detailed description of the DEM generation within the Geomatica software. The geometric model being used is a rigorous one; it reflects the physical reality of the complete viewing geometry and corrects distortions that occur in the imaging process due to platform, sensor, earth, and cartographic projection conditions. After rigorous models (collinearity and coplanarity equations) are computed for the 3N and 3B images, a pair of quasi-epipolar images is generated from the images in order to retain elevation parallax in only one direction. An automated image-matching procedure is used to generate the DEM through a comparison of the respective gray values of these images.

As ground control points (GCPs) were not available, 23 tie points

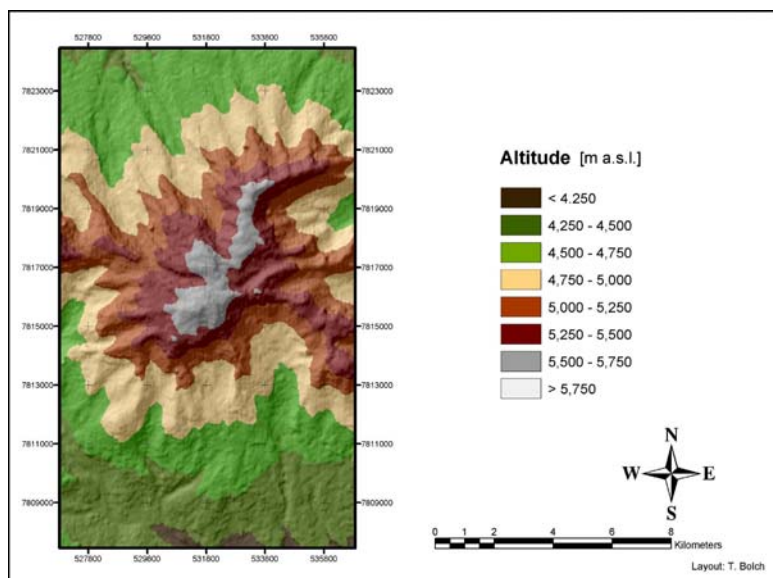


Fig. 3: The digital elevation model (DEM) derived from ASTER satellite data of Cerro Sillajhuay, representing elevation in eight classes. (See also Fig. 5).

(TPs) were collected between the stereo-pair. For 11 TPs the elevation value was known. The total RMS of the TPs was < 1.17 pixel. The DEM was generated at 30 m resolution with the highest possible level of detail, and the holes were filled by automated interpolation. The overall quality of the DEM was outstanding, with only few artifacts mostly representing lakes. The DEM was re-sampled to 15 m to exploit full ortho-image resolution (Fig. 3).

The three-band VNIR nadir-looking image (1, 2, 3N) was orthorectified using the extracted DEM. Several perspective scenes and ‘fly-by’ simulations were developed showing the Cerro Sillaj-huay from different views and in different scales (Fig. 4).

Although GCPs were not available, the absolute elevation of the ASTER DEM is of good accuracy and allows analysis of the macro- and mesorelief. In the altitudes above 5500 m asl., elevation values are low, due to the internal smoothing procedures of the Geomatica software. ASTER DEMs in general are known to be often too low (personal communication, PCI). Nevertheless, the developed 3D-views demonstrate the high quality of the DEM and the potential for more detailed image interpretation.

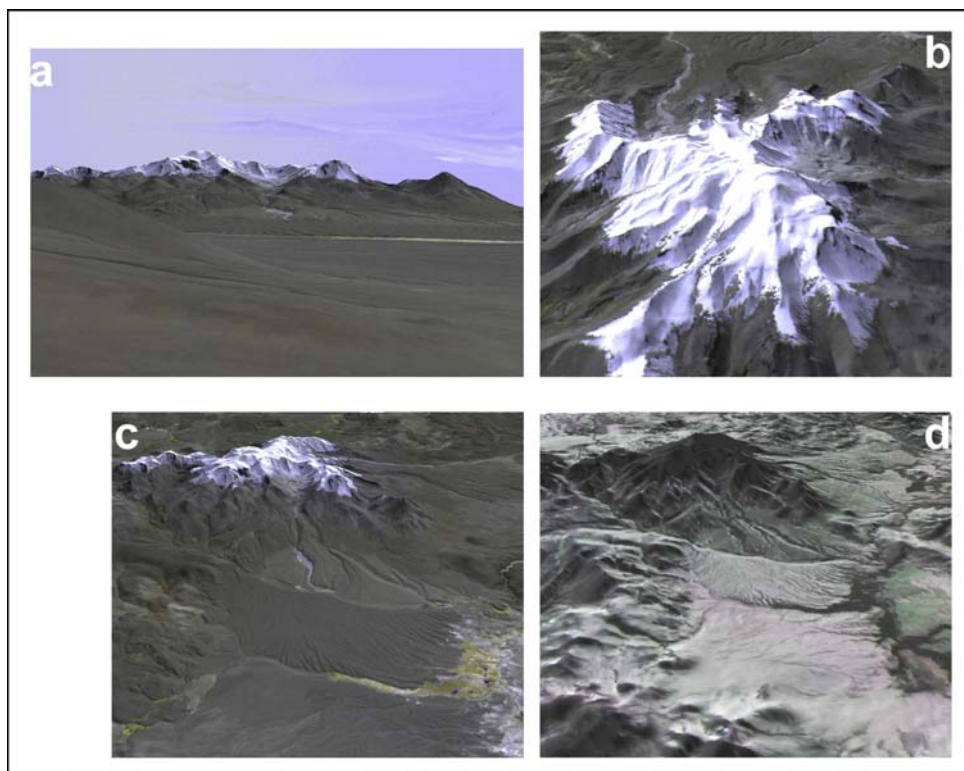


Fig. 4: Virtual 3D-views using of the ASTER DEM of Cerro Sillajhuay. Compare the virtual simulation in (a) with the photograph in Fig. 2; (d) shows a TIR canal combination.

GEOMORPHOMETRIC ANALYSIS

Five geomorphic parameters, which are useful to identify and describe geomorphologic forms and processes, were extracted using the software ArcInfo and ArcView: elevation, aspect, slope angle, vertical curvature, and tangential curvature. Flow lines and the catchment areas of the rock glaciers were extracted using the ‘hydrologic modeling’ tool of the ArcView software. The yearly mean solar radiation was computed using the software SAGA developed by Böhner et al. (1997), which enables an integration of the water vapor content in the atmosphere and the atmospheric pressure.

The elevation is graphically presented in a hypsometric map with eight classes, which at Cerro Sillajhuay at the same time represent altitudinal belts (Fig. 3), e.g. the green class is vegetation cover, the yellow class is a transition zone, and the gray class represents firn fields. In general the ASTER DEM is too low if compared with reality: the summit is only at 5745 m asl. (reality: 5982 m asl.), and the mean altitude is only 4842 m asl. (reality: ~ 4930 m asl.). This fact is mainly caused by the lack of GCPs and smoothing procedures of the Geomatica software.

Topography can be generalized into eight aspect classes, and this may also help to identify geomorphologic features (Fig. 5a). For example, differences in aspect may be an indicator of valley asymmetry.

Another map demonstrates the slope angle in ten classes (Fig. 5b). The class with the lowest slope has a relatively steep upper boundary (5°) in accordance with the general relief, which comprises nearly no flat areas. Other slope classes may be useful to identify specific geomorphic forms: for example, rectilinear slopes (German: 'Glatthänge') have a slope of 25-35° per definition and should be found in the corresponding two classes of the slope map.

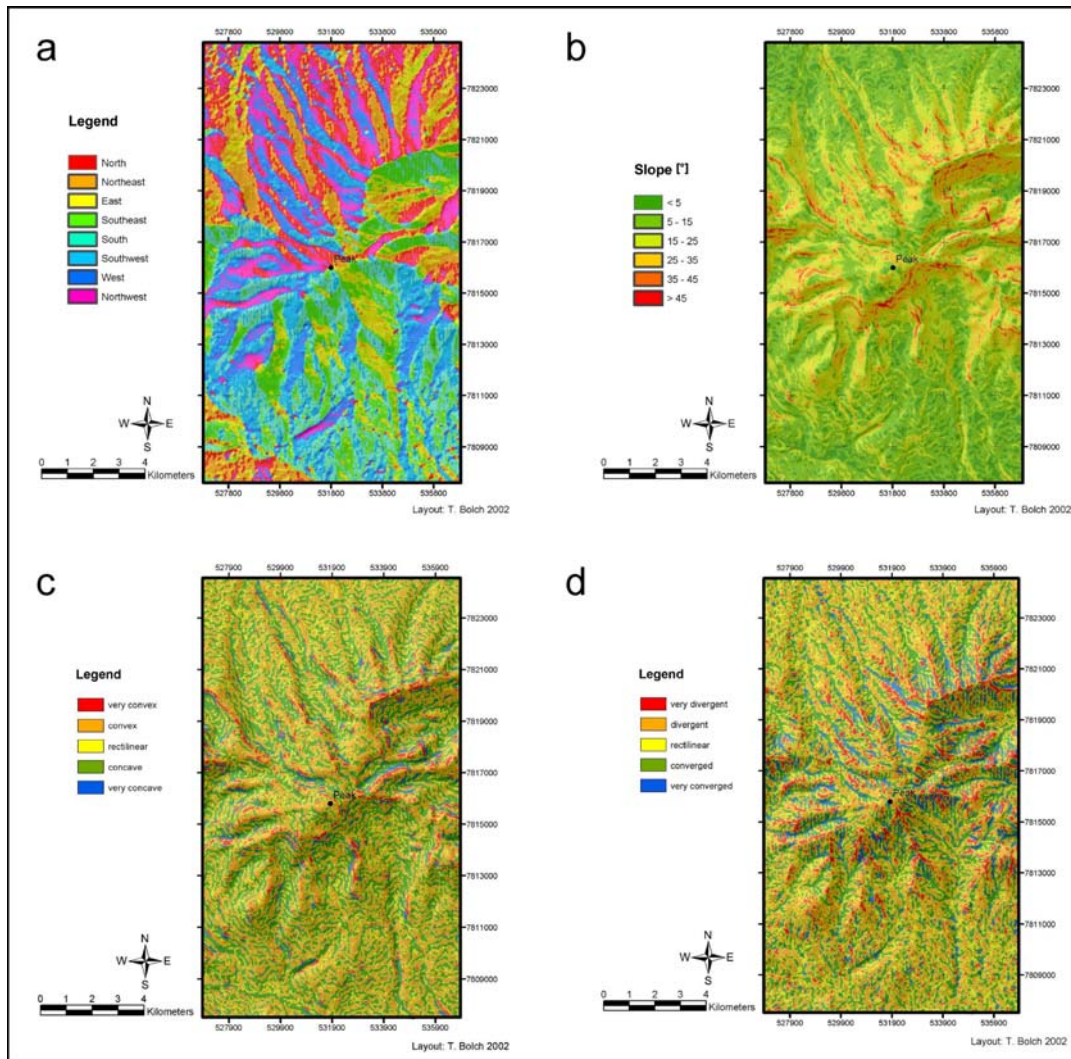


Fig. 5: Morphometric parameters of Cerro Sillajhuay deriving from the ASTER DEM: (a) aspect, (b) slope angle, (c) vertical curvature, (d) tangential curvature. (For elevation see Fig. 3).

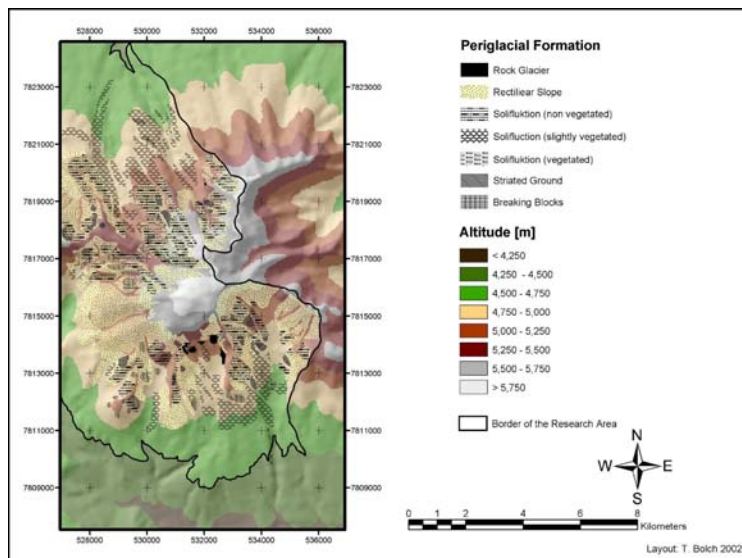


Fig. 6: Periglacial map of Cerro Sillajhuay derived from inter-pretation of the ASTER DEM and field data.

Slope curvature is of special interest for morphological and hydro-logical problems. Both curvatures are shown in maps of five classes: The vertical curvature is the second derivation of elevation regarding slope (Fig. 5c); and the tangential curvature is the second derivation of elevation relating to aspect (Fig. 5d). Obviously, ridges have (very)

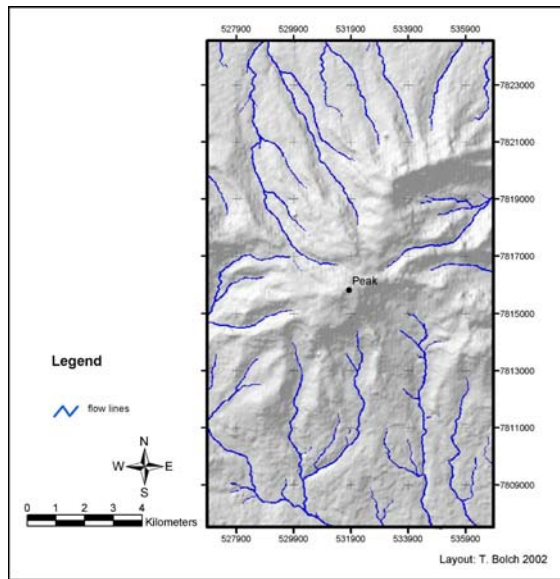


Fig. 7: Map showing the flow lines of Cerro Sillajhuay using the ASTER DEM.

convex and divergent profiles, and valleys have mostly (very) concave and convergent profiles. Mesoscale objects such as rock glaciers can be identified in several locations; the rock glacier front is characterized by a convex profile curvature and convex tangential curvature. In general, profile and tangential curvature are realistic even though the ASTER DEM contains a few artifacts caused by perspective.

Table 1: Areas of periglacial forms calculated from the ASTER DEM.

| Periglacial Form | Covered Area in % |
|---------------------------------|-------------------|
| Rectilinear Slopes | 35 |
| Rock Glacier | 0.3 |
| Non-vegetated Solifluction | 11 |
| Slightly vegetated Solifluction | 10 |
| Vegetated Solifluction | 0.1 |
| Striated and Patterned Grounds | 1.5 |
| Breaking Blocks | 2.5 |
| Firn | 2.0 |

A special interest of the study was a focus on the periglacial forms at Cerro Sillajhuay. A periglacial map could be produced using the DEM (Fig. 6), and the area of each periglacial form was calculated (Table 1). Recti-linear slopes cover most of the study area. Non-vegetated solifluction mainly appears on the rectilinear slopes; slightly vegetated solifluction reaches up to the lower limit of the rectilinear slopes; and vegetated solifluction is very exceptionally. Also, rock glaciers occur very rarely in general, but in some valleys they may cover up to 5 % of the area. Striated and patterned ground, breaking blocks, and firn cover smaller areas.

A more detailed analysis was undertaken for the rock glaciers in the Tacurma Valley. Knowledge about the geomorphometry is also important for a hydrologic modeling. The more accurate the DEM the better the modeling results. Flow lines and surface run-off were calculated to delimit the catchment areas of the rock glaciers. The ASTER DEM seems to be precisely regarding the flow lines by comparing it with the virtual image (Fig. 7). The surface run-off shows very good results especially for the most active rock glaciers.

SOLAR RADIATION

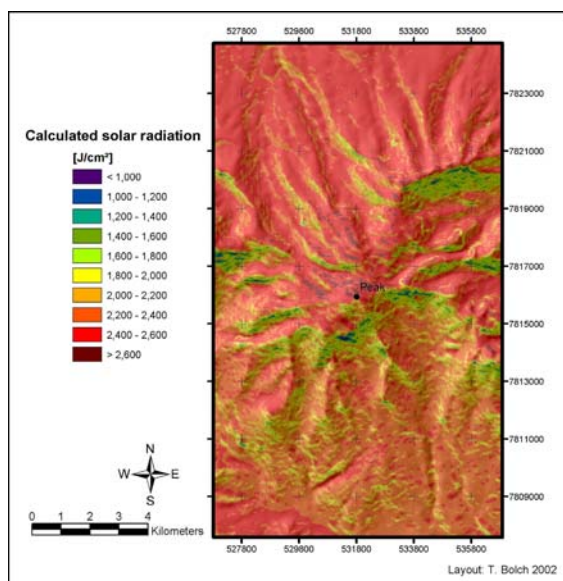


Fig. 8: Map of the solar radiation at Cerro Sillajhuay derived from the ASTER DEM.

In the study area, the solar radiation is of special interest as some authors suppose that the Atacama may have the highest solar radiation rates on Earth. Schmidt (1999) mentions radiation values of 95 % of the solar constant for ca. 3700 m asl., and of 98 % at the Sairecabur, a volcano in northern Chile (5971 m asl., 22°43'S / 67°53'W). The reasons for these high values are low latitude, high elevation, dryness, and lack of nearly any clouds. Radiation values were calculated using the software SAGA developed by Böhner et al. (1997), which integrates the water vapor content in the atmosphere and the atmospheric pressure.

In the map of solar radiation, areas of high radiation are easy to differentiate from areas of low radiation (Fig. 8). It is plausibly that northern slopes receive higher radiation rates than southern slopes. The influence of the relief is plainly recognizable: the highest values appear on the summit, which is nearly always exposed to the sun; the lowest rates can be found at southern exposed escarpments and the large field of permanent snow. The

lowest rates were calculated for steep slopes, and the highest rates for slope angles of $\sim 15^\circ$. These values correlate with field measurements. For the 21 June and 23 December absolute radiation values were calculated: the maximum value is just above 3000 J/cm^2 on 21 June and $\sim 3600 \text{ J/cm}^2$ on 23 December; the minimum value is $\sim 2000 \text{ J/cm}^2$ on 21 December. On 21 December high rates can be found on slightly sloping surfaces such as the summit area, ridges, valley bottoms, and pediments. For rock glaciers and especially their catchment areas, the relatively low minimum daily solar radiation rates for steep slopes calculated with the help of the ASTER DEM are reliable.

DISCUSSION

While developing an ASTER DEM by using a special commercial software package, the DEM developing algorithm cannot be changed easily. Often, the software offers only a few parameters for free selection by the operator. For identifying TPs, the operator needs experience in landforms and land covers, because the quality of the TPs is essential for the DEM quality. But when familiar with the software, an operator can develop an ASTER DEM relatively quickly. ASTER DEMs are excellent for virtual-reality visualisations, because they represent quasi ortho-images.

The Algorithm Theoretical Basis Document for ASTER Digital Elevation Models (Version 3.0, Lang & Welch 1999) suggests that RMSEz values for ASTER DEMs should be on the order of 10 to 50 meters. DEMs produced in other mountainous areas have a preferential failure mode, that is, facets with an aspect of $340 - 140$ degrees or slopes over 35 degrees. This is likely due to two factors. First, relative to the ground being examined, the aft looking ASTER sensor is set at an azimuth of roughly 10 degrees, making slopes with an aspect of 10 degrees the least likely to be well imaged. Second, these slopes receive the least direct solar illumination, which, by reducing image contrast, increases the probability of image-to-image correlation failure.

CONCLUSION

For Cerro Sillajhuay, a volcano in the Andes of Chile/Bolivia, a DEM was developed using ASTER remote sensing data. The results presented here demonstrate that the DEM is useful for morphometric analysis. The scale of a DEM sets the limits for the level of detail for geomorphologic analysis. Today, DEMs from ASTER remote sensing data are reliable sources for an interpretation of the macro- and mesorelief. ASTER DEMs offer relatively great detail, are often easy to develop, and available for many parts of the Earth. The actual purchase price (December 2002) of an ASTER scene is \$55. In general, the ASTER DEM is accurate, e.g. cliff faces and steep slopes are easy to identify. Analyzing the microrelief requires a level of detail, which today's DEM resolutions deriving from satellite data do not offer. Here, aerial photographs still are the better choice.

ASTER data provides the opportunity for mapping at medium scales (1:100,000 and 1:50,000), and for extracting elevation information from nadir and aft images. The simultaneous along-track stereo data eliminates radiometric variations caused by multi-date stereo data acquisition while improving image-matching performance. In cases where precise GCPs cannot be obtained, it is possible to generate DEMs through TPs alone.

ACKNOWLEDGEMENTS

The authors like to thank J. Böhner, University of Göttingen, for solar radiation calculations.

REFERENCES

- Abrams, M. and Hook, S.J. (1995): Simulated ASTER data for geological studies. *IEEE Transactions on Geoscience and Remote Sensing*, 33: 692-699.
- Al-Rousan, N., Cheng, P., Petrie, G., Toutin, T. and Valadan Zoej, M.J. (1997): Automated DEM extraction and orthoimage generation from SPOT level 1B imagery. *Photogrammetric Engineering and Remote Sensing*, 63: 965-974.
- Baral, D.J. and Gupta, R.P. (1997): Integration of satellite sensor data with DEM for the study of snow cover distribution and depletion pattern. *International Journal of Remote Sensing*, 18: 3889-3894.
- Bishop, M.P., Bonk, R., Kamp, U. and Shroder, J.F. (2001): Topographic analysis and modeling for alpine glacier mapping. *Polar Geography*, 25: 182-201 .

- Bishop, M.P. and Shroder, J.F. (2000): Remote sensing and geomorphometric assessment of topographic complexity and erosion dynamics in the Nanga Parbat massif. In: Khan, M.A., Treloar, P.J., Searle, M.P. and Jan, M.Q. (Eds.), *Tectonics of the Nanga Parbat Syntax and the Western Himalaya* (= Geological Society London, Special Publications, 170), London, pp. 181-199.
- Böhner, J., Köthe, R. and Trachinow, C. (1997): Weiterentwicklung der automatischen Relieffanalyse auf der Basis von digitalen Geländemodellen. *Göttinger Geographische Arbeiten*, 100: 3-21.
- Bolch, T. and Schröder, H. (2001): *Geomorphologische Kartierung und Diversitätsbestimmung der Periglazialformen am Cerro Sillajhuay (Chile/Bolivien)*. (= Erlanger Geographische Arbeiten, 28), Erlangen, 141 pp.
- Cheng, P. and McBean, L. (2002): Fly-through data generation of Afghanistan. *Earth Observation Magazine*, without page.
- Desmet, P.J.J. and Govers, G. (1995): GIS-based simulation of erosion and deposition patterns in an agricultural landscape: a comparison of model results with soil map information. *Catena*, 25: 389-401.
- Dietrich, W.E., Wilson, C.J., Montgomery, D.R. and McKean, J. (1993): Analysis of erosion thresholds, channel networks, and landscape morphology using a digital terrain model. *Journal of Geology*, 101: 259-278.
- Dikau, R., Brabb, E.E., Mark, R.K. and Pike, R.J. (1995): Morphometric landform analysis of New Mexico. *Zeitschrift für Geomorphologie, N.F., Suppl.-Bd.*, 101: 109-126.
- Duncan, C.C., Klein, A.J., Masek, J.G. and Isacks, B.L. (1998): Comparison of Late Pleistocene and modern glacier extents in central Nepal based on digital elevation data and satellite imagery. *Quaternary Research*, 49: 241-254.
- Etzelmüller, B. and Sollid, J.L. (1997): Glacier geomorphometry - an approach for analysing long-term glacier surface changes using grid-based digital elevation models. *Annals of Glaciology*, 24: 135-141.
- Giles, P.T. (1998): Geomorphological signatures: classification of aggregated slope unit objects from digital elevation and remote sensing data. *Earth Surface Processes and Landforms*, 23: 581-594.
- Kirkby, M.J. (1990): The landscape viewed through models. *Zeitschrift für Geomorphologie, N.F., Suppl.-Bd.*, 79: 63-81.
- Kneisel, C., Lehmkuhl, F., Winkler, S., Tressel, E. and Schröder, H. (1998): Legende für geomorphologische Kartierungen in Hochgebirgen (GMK Hochgebirge). *Trierer Geographische Studien*, 18: 1-24.
- Krzystek, P. (1995): New investigations into the practical performance of automatic DEM generation. *Proceedings, ACSM/ASPRS Annual Convention, Charlotte, North Carolina, American Society for Photogrammetry and Remote Sensing*, 2, pp. 488-500.
- Lang, H.R. and Welch, R. (1999): Algorithm Theoretical Basis Document for ASTER Digital Elevation Models (Standard Product AST14) Version 3.0. *NASA EOS Publication ATBD-AST-08*.
- Lodwick, G.D. and Paine, S.H. (1985): A digital elevation model of the Barnes Ice-Cap derived from Landsat MSS data. *Photogrammetric Engineering and Remote Sensing*, 51: 1937-1944.
- Millaresis, G.C. and Argialas, D.P. (2000): Extraction and delineation of alluvial fans from digital elevation models and Landsat Thematic Mapper images. *Photogrammetric Engineering and Remote Sensing*, 66: 1093-1101.
- Raup, B.H., Kieffer, H.H., Hare, T.M. and Kargel, J.S. (2000): Generation of data acquisition requests for the ASTER satellite instrument for monitoring a globally distributed target: Glaciers. *IEEE Transactions on Geoscience and Remote Sensing*, 38: 1105-1112.
- Rickenbacher, M. (1998): Die digitale Modellierung des Hochgebirges im DGM25 des Bundesamtes fuer Landestopographie. *Wiener Schriften zur Geographie und Kartographie*, 11: 49-55.
- Röttger, S., Heidrich, W., Slusallek, P. and Seidel, H.-P. (1998): Real-time generation of continuous levels of detail for height fields. *Proceedings Sixth International Conference in Central Europe on Computer Graphics and Visualization, Plzen, Czech Republic*, pp. 315-322.
- Schmidt, D. (1999): *Das Extremklima der nordchilenischen Hochatacama unter besonderer Berücksichtigung der Höhengradienten*. (= Dresdner Geographische Beiträge, 4), Dresden, 122 pp.
- Schneider (1998): *Geomorphologisch plausible Rekonstruktion der digitalen Repräsentation von Geländeoberflächen aus Höhendaten*. Unpublished Dissertation, Universität Zürich, Schweiz, 226 pp.
- Schröder, H., Bolch, T. and Kröber, G. (1999): Limnische Sedimentationen des Holozäns im Becken von Cancosa (Provinz Iquique, Chile). *Mitteilungen der Fränkischen Geographischen Gesellschaft*, 46: 217-229.
- Schröder, H. and Makki, M. (1998): Das Periglazial des Llullaillaco (Chile/Argentinien). *Petermanns Geographische Mitteilungen*, 142: 67-84.
- Schröder, H. and Schmidt, D. (1997): Klimamorphologie und Morphogenese des Llullaillaco (Chile/Argentinien). *Mitteilungen der Fränkischen Geographischen Gesellschaft*, 44: 225-258.
- Sidjak, R.W. and Wheate, R.D. (1999): Glacier mapping of the Illecillewaet icefield, British Columbia, Canada, using Landsat TM and digital elevation data. *International Journal of Remote Sensing*, 20: 273-284.
- Shi, J. (2001): Estimation of snow fraction using simulated ASTER data. *IAHS Publication*, 267: 120-122.

- Tucker, G.E., Catani, F., Rinaldo, A. and Bras, R.L. (2001): Statistical analysis of drainage density from digital terrain data. *Geomorphology*, 36, 187-202.
- Welch, R., Jordan, T., Lang, H. and Murakami, H. (1998): ASTER as a source for topographic data in the late 1990's. *IEEE Transactions on Geoscience and Remote Sensing*, 36: 1282-1289.
- Wessels, R.L., Kargel, J.S. and Kieffer, H.H. (2002): ASTER measurement of supraglacial lakes in the Mount Everest region of the Himalaya. *Annals of Glaciology*, 34: 399-408.